Smart Structures Systems, *Vol. 19, No. 4 (2017) 441-448*
DOI: https://doi.org/10.12989/sss.2017.19.4.441

Analysis of functionally graded plates using a sinusoidal shear deformation theory

Lazreg Hadji*[1,2]

[1]*Departement de Genie Civil, Universite Ibn Khaldoun, BP 78 Zaaroura, 14000 Tiaret, Algerie*
[2]*Laboratoire des Materiaux & Hydrologie, Universite de Sidi Bel Abbes, 22000 Sidi Bel Abbes, Algerie*

(Received July 16, 2016, Revised January 9, 2017, Accepted January 13, 2017)

Abstract. This paper uses the four-variable refined plate theory for the free vibration analysis of functionally graded material (FGM) rectangular plates. The plate properties are assumed to be varied through the thickness following a simple power law distribution in terms of volume fraction of material constituents. The theory presented is variationally consistent, does not require shear correction factor, and gives rise to transverse shear stress variation such that the transverse shear stresses vary parabolically across the thickness satisfying shear stress free surface conditions. Equations of motion are derived from the Hamilton's principle. The closed-form solutions of functionally graded plates are obtained using Navier solution. Numerical results of the refined plate theory are presented to show the effect of the material distribution, the aspect and side-to-thickness ratio on the fundamental frequencies. It can be concluded that the proposed theory is accurate and simple in solving the free vibration behavior of functionally graded plates.

Keywords: Navier's solutions; functionally graded material (FGM); free vibration; theoretical formulation

1. Introduction

Functionally graded materials (FGMs) are a class of composites that have continuous variation of material properties from one surface to another, and thus eliminating the stress concentration found in laminated composites. A typical FGM is made from a mixture of ceramic and metal. These materials are often isotropic but nonhomogeneous. The reason for interest in FGMs is that it may be possible to create certain types of FGM structures capable of adapting to operating conditions.

Due to the increased relevance of the FGMs structural components in the design of engineering structures, many studies have been reported on the vibration analyses of functionally graded (FG) plates. Thai *et al*. (2013a) used a simple quasi-3D sinusoidal shear deformation theory for functionally graded plates. Thai *et al*. (2013b) proposed a simple higher-order shear deformation theory for bending and free vibration analysis of functionally graded plates. Zhang *et al*. (2013) studied the modeling and analysis of FGM rectangular plates based on physical neutral surface and high order shear deformation theory. Fekrar *et al*. (2012) analyzed the buckling response of FG hybrid composite plates using a new four variable refined plate theory. Tai *et al*. (2014) studied the analysis of functionally graded sandwich plates using a new first-order shear deformation theory. Bousahla *et al*. (2014) investigated a novel higher order shear and normal deformation theory based on neutral surface position for bending analysis of advanced composite plates. Belabed *et al*. (2014) used an efficient and simple higher order shear and normal deformation theory for functionally graded material (FGM) plates. Ait Amar Meziane *et al*. (2014) used an efficient and simple refined theory for buckling and free vibration of exponentially graded sandwich plates under various boundary conditions. Mahi *et al*. (2015) developed a new hyperbolic shear deformation theory for bending and free vibration analysis of isotropic, functionally graded, sandwich and laminated composite plates. Bellifa *et al*. (2016) studied the bending and free vibration analysis of functionally graded plates using a simple shear deformation theory and the concept the neutral surface position. Al-Basyouni *et al*. (2015) investigated size dependent bending and vibration analysis of functionally graded micro beams based on modified couple stress theory and neutral surface position. Belkorissat *et al*. 2015) developed new shear deformation plates theories involving only four unknown functions. Larbi Chaht *et al*. (2015) studied the bending and buckling of functionally graded material (FGM) size-dependent nanoscale beams including the thickness stretching effect. Ahouel *et al*. (2016) investigated a size-dependent mechanical behavior of functionally graded trigonometric shear deformable nanobeams including neutral surface position concept. Zemri *et al*. (2015) proposed an assessment of a refined nonlocal shear deformation theory beam theory for a mechanical response of functionally graded nanoscale beam. Nedri *et al*. (2014) developed new shear deformation plate theorie involving only four unknown functions for free vibration analysis of laminated composite plates resting on elastic foundations.
Tounsi *et al*. (2013) used a refined trigonometric shear deformation theory for thermoelastic bending of functionally graded sandwich plates. Zidi *et al*. (2014) study

*Corresponding author, Ph.D.
E-mail: had_laz@yahoo.fr

http://www.techno-press.com/journals/sss&subpage=7
ISSN: 1738-1584 (Print), 1738-1991 (Online)

hygro-thermo-mechanical loading for the bending of FGM plates using a four variable refined plate theory. Bouderba *et al*. (2013) studied the thermomechanical bending response of FGM thick plates resting on Winkler-Pasternak elastic foundations. Bouderba *et al*. (2016) studied the thermal stability of functionally graded sandwich plates using a simple shear deformation theory. Attia *et al*. (2015) developed the free vibration analysis of functionally graded plates with temperature-dependent properties using various four variable refined plate theories. Bakora *et al*. (2015) investigated the thermo-mechanical post-buckling behavior of thick functionally graded plates resting on elastic foundations. Boukhari *et al*. (2016) used an efficient shear deformation theory for wave propagation of functionally graded material plates. Hebali *et al*. (2014) studied the static and free vibration analysis of functionally graded plates using a new quasi-3D hyperbolic shear deformation theory. Hamidi *et al*. (2015) used a sinusoidal plate theory with 5-unknowns and stretching effect for thermomechanical bending of functionally graded sandwich plates. Bourada *et al*. (2015) used a new simple shear and normal deformations theory for functionally graded beams. Hadji *et al*. (2016a) analyze the functionally graded beam using a new first-order shear deformation theory. Bennoun *et al*. (2016) used a novel five variable refined plate theory for vibration analysis of functionally graded sandwich plates. Ait Yahia *et al*. (2015) studied the wave propagation in functionally graded plates with porosities using various higher-order shear deformation plate theories. Beldjelili *et al*. (2016) analyzed the hygro-thermo-mechanical bending of S-FGM plates resting on variable elastic foundations using a four-variable trigonometric plate theory. Hadji *et al*. (2016b) used a new first shear deformation theory for the dynamic behavior of FGM beam. Bounouara *et al*. (2016) studied the free vibration of functionally graded nanoscale plates resting on elastic foundation using a nonlocal zeroth-order shear deformation theory. Hadji *et al*. (2016c) analyzed the bending of FGM plates using a sinusoidal shear deformation theory.

In this paper, a refined shear deformation plate theory which eliminates the use of the shear correction factor is developed for FG plates. By making a further assumption, the number of unknowns and governing equations of the present refined theory is reduced, thus makes it simple to use. Equations of motion and boundary conditions are derived from Hamilton's principle. Analytical solutions for rectangular plates are obtained. Numerical examples are presented to verify the accuracy of the present theory in predicting the free vibration responses of FG plates.

2. Theoretical formulation

Consider a rectangular FGM plate having the thickness h, length a, and width b. A Cartesian coordinate system (*x*, *y*, *z*) is used to label the material point of the plate in the unstressed reference configuration, as depicted in Fig. 1. It is assumed that the material is isotropic and grading is assumed to be only through the thickness. The *xy* plane is taken to be the undeformed mid plane of the plate with the *z* axis positive upward from the mid plane.

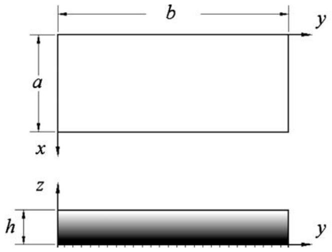

Fig. 1 Geometry of rectangular FG plate and coordinates

2.1 Basic assumptions

The assumptions of the present theory are as follows:

The displacements are small in comparison with the plate thickness and, therefore, strains involved are infinitesimal.

The transverse displacement *W* includes two components of bending w_b, and shear w_s. These components are functions of coordinates x, y, and time t only

$$w(x,y,z,t) = w_b(x,y,t) + w_s(x,y,t) \tag{1}$$

The transverse normal stress σ_z is negligible in comparison with in-plane stresses σ_x and σy.

The displacements U in *x*-direction and V in y-direction consist of extension, bending, and shear components

$$u = u_0 + u_b + u_s \qquad v = v_0 + v_b + v_s \tag{2}$$

The bending components u_b and v_b are assumed to be similar to the displacements given by the classical plate theory. Therefore, the expression for u_b and v_b can be given as

$$u_b = -z\frac{\partial w_b}{\partial x} \qquad v_b = -z\frac{\partial w_b}{\partial y} \tag{3a}$$

The shear components u_s and v_s give rise, in conjunction with w_s, to the parabolic variations of shear strains γ_{xz}, γ_{yz} and hence to shear stresses τ_{xz}, τ_{yz} through the thickness of the plate in such a way that shear stresses τ_{xz}, τ_{yz} are zero at the top and bottom faces of the plate. Consequently, the expression for u_s and v_s can be given as

$$u_b = -z\frac{\partial w_b}{\partial x} \qquad v_b = -z\frac{\partial w_b}{\partial y} \tag{3b}$$

2.2 Displacement fields and strains

Based on the assumptions made in the preceding section, the displacement field can be obtained

$$\begin{aligned} u(x,y,z,t) &= u_0(x,y,t) - z\frac{\partial w_b}{\partial x} - f(z)\frac{\partial w_s}{\partial x} \\ v(x,y,z,t) &= v_0(x,y,t) - z\frac{\partial w_b}{\partial y} - f(z)\frac{\partial w_s}{\partial y} \\ w(x,y,z,t) &= w_b(x,y,t) + w_s(x,y,t) \end{aligned} \tag{4}$$

where u_0 and v_0 are the mid-plane displacements of the plate in the ***x*** and ***y*** direction, respectively; w_b and w_s are the bending and shear components of transverse displacement, respectively.

The kinematic relations can be obtained as follows

$$\begin{aligned}\varepsilon_x &= \varepsilon_x^0 + z\,k_x^b + f\,k_x^s\\ \varepsilon_y &= \varepsilon_y^0 + z\,k_y^b + f\,k_y^s\\ \gamma_{xy} &= \gamma_{xy}^0 + z\,k_{xy}^b + f\,k_{xy}^s\\ \gamma_{yz} &= g\,\gamma_{yz}^s\\ \gamma_{xz} &= g\,\gamma_{xz}^s\\ \varepsilon_z &= 0\end{aligned} \tag{5}$$

where

$$\begin{cases}\varepsilon_x^0 = \dfrac{\partial u_0}{\partial x}, k_x^b = -\dfrac{\partial^2 w_b}{\partial x^2},\ k_x^s = -\dfrac{\partial^2 w_s}{\partial x^2}\\ \varepsilon_y^0 = \dfrac{\partial v_0}{\partial y}, k_y^b = -\dfrac{\partial^2 w_b}{\partial y^2}, k_y^s = -\dfrac{\partial^2 w_s}{\partial y^2}\\ \gamma_{xy}^0 = \dfrac{\partial u_0}{\partial y} + \dfrac{\partial v_0}{\partial x}, k_{xy}^b = -2\dfrac{\partial^2 w_b}{\partial x \partial y}, k_{xy}^s = -2\dfrac{\partial^2 w_s}{\partial x \partial y}\\ \gamma_{yz}^s = \dfrac{\partial w_s}{\partial y}, \gamma_{xz}^s = \dfrac{\partial w_s}{\partial x}\\ g(z) = 1 - f'(z)\ \ and\ \ f'(z) = \dfrac{df(z)}{dz}\end{cases}$$

$$\varepsilon_x^0 = \frac{\partial u}{\partial x},\quad k_x^b = -\frac{\partial^2 w_b}{\partial x^2},\quad k_x^s = -\frac{\partial^2 w_s}{\partial x^2} \tag{6}$$

$$\varepsilon_y^0 = \frac{\partial v}{\partial y},\quad k_y^b = -\frac{\partial^2 w_b}{\partial y^2},\quad k_y^s = -\frac{\partial^2 w_s}{\partial y^2}$$

$$\gamma_{xy}^0 = \frac{\partial u}{\partial y} + \frac{\partial v}{\partial x},\quad k_{xy}^b = -2\frac{\partial^2 w_b}{\partial x \partial y},\quad k_{xy}^s = -2\frac{\partial^2 w_s}{\partial x \partial y}$$

$$\gamma_{yz}^s = \frac{\partial w_s}{\partial y},\quad \gamma_{xz}^s = \frac{\partial w_s}{\partial x}$$

$$g(z) = 1 - f'(z) \text{ and } f'(z) = \frac{df(z)}{dz}$$

while $f(z)$ represents shape functions determining the distribution of the transverse shear strains and stresses along the thickness and is given as

$$f(z) = z - \frac{\pi}{h}\sin\left(\frac{\pi z}{h}\right) \tag{7}$$

2.3 Constitutive relations

The material properties of FG plate are assumed to vary continuously through the thickness of the plate in accordance with a power law distribution as

$$P(z) = P_b + (P_t - P_b)\left(\frac{z}{h} + \frac{1}{2}\right)^k \tag{8}$$

Where P denotes a generic material property like modulus, P_t and P_b denotes the property of the top and bottom faces of the plate respectively, and k is a parameter that dictates material variation profile through the thickness. Here, it is assumed that modules E and G vary according to the Eq. (8) and ν is assumed to be a constant. The linear constitutive relations of a FG plate can be written as

$$\begin{Bmatrix}\sigma_x\\ \sigma_y\\ \tau_{xy}\end{Bmatrix} = \begin{bmatrix}Q_{11} & Q_{12} & 0\\ Q_{12} & Q_{22} & 0\\ 0 & 0 & Q_{66}\end{bmatrix}\begin{Bmatrix}\varepsilon_x\\ \varepsilon_y\\ \gamma_{xy}\end{Bmatrix} \text{ and}$$

$$\begin{Bmatrix}\tau_{yz}\\ \tau_{zx}\end{Bmatrix} = \begin{bmatrix}Q_{44} & 0\\ 0 & Q_{55}\end{bmatrix}\begin{Bmatrix}\gamma_{yz}\\ \gamma_{zx}\end{Bmatrix} \tag{9}$$

where

$$\begin{aligned}Q_{11} &= Q_{22} = \frac{E(z)}{1-\nu^2}\\ Q_{12} &= \frac{\nu\,E(z)}{1-\nu^2}\\ Q_{44} &= Q_{55} = Q_{66} = \frac{E(z)}{2(1+\nu)}\end{aligned} \tag{10}$$

2.4 Governing equations

Hamilton's principle is used herein to derive the equations of motion appropriate to the displacement field and the constitutive equations. The principle can be stated in analytical form as

$$0 = \int_0^T (\delta U - \delta K)\,dt \tag{11}$$

where δU is the variation of strain energy; and δK is the variation of kinetic energy. The variation of strain energy is calculated by

$$\begin{aligned}\delta U &= \int_\Omega \int_{-\frac{h}{2}}^{\frac{h}{2}} \left[\sigma_x \delta\varepsilon_x + \sigma_y \delta\varepsilon_y + \tau_{xy}\delta\gamma_{xy} + \tau_{yz}\delta\gamma_{yz} + \tau_{xz}\delta\gamma_{xz}\right] dz d\Omega\\ &= \int_\Omega \big[N_x \delta\varepsilon_x^0 + N_y \delta\varepsilon_y^0 + N_{xy}\delta\varepsilon_{xy}^0 + M_x^b \delta k_x^b + M_y^b \delta k_y^b + M_{xy}^b \delta k_{xy}^b + M_x^s \delta k_x^s\\ &\quad + M_y^s \delta k_y^s + M_{xy}^s \delta k_{xy}^s + S_{yz}^s \delta\gamma_{yz}^s + S_{xz}^s \delta\gamma_{xz}^s\big] d\Omega\end{aligned} \tag{12}$$

where Ω is the top surface and N, M, and S are stress resultants defined by

$$\begin{Bmatrix}N_x, & N_y, & N_{xy}\\ M_x^b, & M_y^b, & M_{xy}^b\\ M_x^s, & M_y^s, & M_{xy}^s\end{Bmatrix} = \int_{-\frac{h}{2}}^{\frac{h}{2}} (\sigma_x, \sigma_y, \tau_{xy}) \begin{Bmatrix}1\\ z\\ f(z)\end{Bmatrix} dz, \tag{13a}$$

$$\left(S_{xz}^{s}, S_{yz}^{s}\right) = \int_{-\frac{h}{2}}^{\frac{h}{2}} \left(\tau_{xz}, \tau_{yz}\right) g(z)\, dz \tag{13b}$$

The variation of kinetic energy can be written as

$$\begin{aligned}
\delta K &= \int_{-\frac{h}{2}}^{\frac{h}{2}} \int_{\Omega} \left[\dot{u}\,\delta\dot{u} + \dot{v}\,\delta\dot{v} + \dot{w}\,\delta\dot{w}\right] \rho(z)\, d\Omega\, dz \\
&= \int_A \Big\{ I_1 \left[\dot{u}_0 \delta\dot{u}_0 + \dot{v}_0 \delta\dot{v}_0 + \left(\dot{w}_b + \dot{w}_s\right)\left(\delta\dot{w}_b + \delta\dot{w}_s\right)\right] \\
&- I_2 \left(\dot{u}_0 \frac{\partial \delta\dot{w}_b}{\partial x} + \frac{\partial \dot{w}_b}{\partial x} \delta\dot{u}_0 + \dot{v}_0 \frac{\partial \delta\dot{w}_b}{\partial y} + \frac{\partial \dot{w}_b}{\partial y} \delta\dot{v}_0 \right) \\
&- I_4 \left(\dot{u}_0 \frac{\partial \delta\dot{w}_s}{\partial x} + \frac{\partial \dot{w}_s}{\partial x} \delta\dot{u}_0 + \dot{v}_0 \frac{\partial \delta\dot{w}_s}{\partial y} + \frac{\partial \dot{w}_s}{\partial y} \delta\dot{v}_0 \right) \\
&+ I_3 \left(\frac{\partial \dot{w}_b}{\partial x} \frac{\partial \delta\dot{w}_b}{\partial x} + \frac{\partial \dot{w}_b}{\partial y} \frac{\partial \delta\dot{w}_b}{\partial y} \right) + I_6 \left(\frac{\partial \dot{w}_s}{\partial x} \frac{\partial \delta\dot{w}_s}{\partial x} + \frac{\partial \dot{w}_s}{\partial y} \frac{\partial \delta\dot{w}_s}{\partial y} \right) \\
&+ I_5 \left(\frac{\partial \dot{w}_b}{\partial x} \frac{\partial \delta\dot{w}_s}{\partial x} + \frac{\partial \dot{w}_s}{\partial x} \frac{\partial \delta\dot{w}_b}{\partial x} + \frac{\partial \dot{w}_b}{\partial y} \frac{\partial \delta\dot{w}_s}{\partial y} + \frac{\partial \dot{w}_s}{\partial y} \frac{\partial \delta\dot{w}_b}{\partial y} \right) \Big\} d\Omega
\end{aligned} \tag{14}$$

where dot-superscript convention indicates the differentiation with respect to the time variable t; and (I_1, I_2, I_3, I_4, I_5, I_6) are mass inertias defined as

$$\left(I_1, I_2, I_3, I_4, I_5, I_6\right) = \int_{-\frac{h}{2}}^{\frac{h}{2}} \left(1, z, f, z^2, z\, f, f^2\right) \rho(z)\, dz \tag{15}$$

Substituting the expressions for δU and δK from Eqs. (12) and (14) into Eq. (11a) and integrating by parts, and collecting the coefficients of δu_0, δv_0, δw_b, and δw_s, one obtains the following equations of motion

$$\begin{aligned}
\delta u_0 &: \frac{\partial N_x}{\partial x} + \frac{\partial N_{xy}}{\partial y} = I_1 \ddot{u}_0 - I_2 \frac{\partial \ddot{w}_b}{\partial x} - I_4 \frac{\partial \ddot{w}_s}{\partial x} \\
\delta v_0 &: \frac{\partial N_{xy}}{\partial x} + \frac{\partial N_y}{\partial y} = I_1 \ddot{v}_0 - I_2 \frac{\partial \ddot{w}_b}{\partial y} - I_4 \frac{\partial \ddot{w}_s}{\partial y} \\
\delta w_b &: \frac{\partial^2 M_x^b}{\partial x^2} + 2\frac{\partial^2 M_{xy}^b}{\partial x \partial y} + \frac{\partial^2 M_y^b}{\partial y^2} = I_1\left(\ddot{w}_b + \ddot{w}_s\right) + I_2\left(\frac{\partial \ddot{u}_0}{\partial x} + \frac{\partial \ddot{v}_0}{\partial y}\right) - I_3 \nabla^2 \ddot{w}_b - I_5 \nabla^2 \ddot{w}_s \\
\delta w_s &: \frac{\partial^2 M_x^s}{\partial x^2} + 2\frac{\partial^2 M_{xy}^s}{\partial x \partial y} + \frac{\partial^2 M_y^s}{\partial y^2} + \frac{\partial S_{xz}^s}{\partial x} + \frac{\partial S_{yz}^s}{\partial y} = I_1\left(\ddot{w}_b + \ddot{w}_s\right) + I_4\left(\frac{\partial \ddot{u}_0}{\partial x} + \frac{\partial \ddot{v}_0}{\partial y}\right) - I_5 \nabla^2 \ddot{w}_b - I_6 \nabla^2 \ddot{w}_s
\end{aligned} \tag{16}$$

Using Eq. (9) in Eq. (13), the stress resultants of a plate can be related to the total strains by

$$\begin{Bmatrix} N \\ M^b \\ M^s \end{Bmatrix} = \begin{bmatrix} A & B & B^s \\ B & D & D^s \\ B^s & D^s & H^s \end{bmatrix} \begin{Bmatrix} \varepsilon \\ k^b \\ k^s \end{Bmatrix}, \qquad \begin{Bmatrix} S_{yz}^s \\ S_{xz}^s \end{Bmatrix} = \begin{bmatrix} A_{44}^s & 0 \\ 0 & A_{55}^s \end{bmatrix} \begin{Bmatrix} \gamma_{yz}^s \\ \gamma_{xz}^s \end{Bmatrix} \tag{15}$$

where

$$N = \left\{N_x, N_y, N_{xy}\right\}^t, \quad M^b = \left\{M_x^b, M_y^b, M_{xy}^b\right\}^t, \quad M^s = \left\{M_x^s, M_y^s, M_{xy}^s\right\}^t, \tag{16a}$$

$$\varepsilon = \left\{\varepsilon_x^0, \varepsilon_y^0, \gamma_{xy}^0\right\}^t, \quad k^b = \left\{k_x^b, k_y^b, k_{xy}^b\right\}^t, \quad k^s = \left\{k_x^s, k_y^s, k_{xy}^s\right\}^t, \tag{16b}$$

$$A = \begin{bmatrix} A_{11} & A_{12} & 0 \\ A_{12} & A_{22} & 0 \\ 0 & 0 & A_{66} \end{bmatrix}, \quad B = \begin{bmatrix} B_{11} & B_{12} & 0 \\ B_{12} & B_{22} & 0 \\ 0 & 0 & B_{66} \end{bmatrix}, \quad D = \begin{bmatrix} D_{11} & D_{12} & 0 \\ D_{12} & D_{22} & 0 \\ 0 & 0 & D_{66} \end{bmatrix} \tag{16c}$$

$$B^s = \begin{bmatrix} B_{11}^s & B_{12}^s & 0 \\ B_{12}^s & B_{22}^s & 0 \\ 0 & 0 & B_{66}^s \end{bmatrix}, \quad D^s = \begin{bmatrix} D_{11}^s & D_{12}^s & 0 \\ D_{12}^s & D_{22}^s & 0 \\ 0 & 0 & D_{66}^s \end{bmatrix}, \quad H^s = \begin{bmatrix} H_{11}^s & H_{12}^s & 0 \\ H_{12}^s & H_{22}^s & 0 \\ 0 & 0 & H_{66}^s \end{bmatrix} \tag{16d}$$

The stiffness coefficients A_{ij} and B_{ij}, etc., are defined as

$$\begin{Bmatrix} A_{11} & D_{11} & B_{11}^s & D_{11}^s & H_{11}^s \\ A_{12} & D_{12} & B_{12}^s & D_{12}^s & H_{12}^s \\ A_{66} & D_{66} & B_{66}^s & D_{66}^s & H_{66}^s \end{Bmatrix} = \int_{-\frac{h}{2}-C}^{\frac{h}{2}-C} Q_{11}\left(1, z, z^2, f(z), z\, f(z), f^2(z)\right) \begin{Bmatrix} 1 \\ \nu \\ \frac{1-\nu}{2} \end{Bmatrix} dz \tag{17a}$$

$$\left(A_{22}, B_{22,}, D_{22}, B_{22}^s, D_{22}^s, H_{22}^s\right) = \left(A_{11}, B_{11}, D_{11}, B_{11}^s, D_{11}^s, H_{11}^s\right) \tag{17b}$$

$$A_{44}^s = A_{55}^s = \int_{-\frac{h}{2}-C}^{\frac{h}{2}-C} \frac{E(z)}{2(1+\nu)} \left[g(z)\right]^2 dz, \tag{17c}$$

Substituting from Eq. (15) into Eq. (16), the equations of motion can be expressed in terms of displacements (δu_0, δv_0, δw_b, δw_s) as

$$\begin{aligned}
&A_{11}\frac{\partial^2 u}{\partial x^2} + A_{66}\frac{\partial^2 u}{\partial y^2} + \left(A_{12} + A_{66}\right)\frac{\partial^2 v}{\partial x \partial y} - B_{11}\frac{\partial^3 w_b}{\partial x^3} - \left(B_{12} + 2B_{66}\right)\frac{\partial^3 w_b}{\partial x \partial y^2} - B_{11}^s \frac{\partial^3 w_s}{\partial x^3} \\
&- \left(B_{12}^s + 2B_{66}^s\right)\frac{\partial^3 w_s}{\partial x \partial y^2} = I_1 \ddot{u}_0 - I_2 \frac{\partial \ddot{w}_b}{\partial x} - I_4 \frac{\partial \ddot{w}_s}{\partial x},
\end{aligned} \tag{18a}$$

$$\begin{aligned}
&\left(A_{12} + A_{66}\right)\frac{\partial^2 u}{\partial x \partial y} + A_{66}\frac{\partial^2 v}{\partial x^2} + A_{22}\frac{\partial^2 v}{\partial y^2} - \left(B_{12} + 2B_{66}\right)\frac{\partial^3 w_b}{\partial x^2 \partial y} - B_{22}\frac{\partial^3 w_b}{\partial y^3} - B_{22}^s \frac{\partial^3 w_s}{\partial y^3} \\
&- \left(B_{12}^s + 2B_{66}^s\right)\frac{\partial^3 w_s}{\partial x^2 \partial y} = I_1 \ddot{v}_0 - I_2 \frac{\partial \ddot{w}_b}{\partial y} - I_4 \frac{\partial \ddot{w}_s}{\partial y}
\end{aligned} \tag{18b}$$

$$B_{11}\frac{\partial^3 u}{\partial x^3}+(B_{12}+2B_{66})\frac{\partial^3 u}{\partial x\partial y^2}+(B_{12}+2B_{66})\frac{\partial^3 v}{\partial x^2\partial y}+B_{22}\frac{\partial^3 v}{\partial y^3}-D_{11}\frac{\partial^4 w_b}{\partial x^4}$$
$$-2(D_{12}+2D_{66})\frac{\partial^4 w_b}{\partial x^2\partial y^2}-D_{22}\frac{\partial^4 w_b}{\partial y^4}-D_{11}^s\frac{\partial^4 w_s}{\partial x^4}-2(D_{12}^s+2D_{66}^s)\frac{\partial^4 w_s}{\partial x^2\partial y^2} \quad (18c)$$
$$-D_{22}^s\frac{\partial^4 w_s}{\partial y^4}=I_1(\ddot{w}_b+\ddot{w}_s)+I_2\left(\frac{\partial \ddot{u}_0}{\partial x}+\frac{\partial \ddot{v}_0}{\partial y}\right)-I_3\nabla^2\ddot{w}_b-I_5\nabla^2\ddot{w}_s,$$

$$B_{11}^s\frac{\partial^3 u}{\partial x^3}+(B_{12}^s+2B_{66}^s)\frac{\partial^3 u}{\partial x\partial y^2}+(B_{12}^s+2B_{66}^s)\frac{\partial^3 v}{\partial x^2\partial y}+B_{22}^s\frac{\partial^3 v}{\partial y^3}-D_{11}^s\frac{\partial^4 w_b}{\partial x^4}$$
$$-2(D_{12}^s+2D_{66}^s)\frac{\partial^4 w_b}{\partial x^2\partial y^2}-D_{22}^s\frac{\partial^4 w_b}{\partial y^4}-H_{11}^s\frac{\partial^4 w_s}{\partial x^4}-2(H_{12}^s+2H_{66}^s)\frac{\partial^4 w_s}{\partial x^2\partial y^2}-H_{22}^s\frac{\partial^4 w_s}{\partial y^4} \quad (18d)$$
$$+A_{55}^s\frac{\partial^2 w_s}{\partial x^2}+A_{44}^s\frac{\partial^2 w_s}{\partial y^2}=I_1(\ddot{w}_b+\ddot{w}_s)+I_4\left(\frac{\partial \ddot{u}_0}{\partial x}+\frac{\partial \ddot{v}_0}{\partial y}\right)-I_5\nabla^2\ddot{w}_b-I_6\nabla^2\ddot{w}_s$$

2.5 Closed-form solution for simply supported plates

Rectangular plates are generally classified according to the type of support used. Here, we are concerned with the exact solutions of Eqs. (18) for a simply supported FG plate. Based on the Navier approach, the solutions are assumed as

$$\begin{Bmatrix} u_0 \\ v_0 \\ w_b \\ w_s \end{Bmatrix}=\sum_{m=1}^{\infty}\sum_{n=1}^{\infty}\begin{Bmatrix} U_{mn}e^{i\omega t}\cos(\lambda x)\sin(\mu y) \\ V_{mn}e^{i\omega t}\sin(\lambda x)\cos(\mu y) \\ W_{bmn}e^{i\omega t}\sin(\lambda x)\sin(\mu y) \\ W_{smn}e^{i\omega t}\sin(\lambda x)\sin(\mu y) \end{Bmatrix} \quad (19)$$

where U_{mn}, V_{mn}, W_{bmn} and W_{smn} are arbitrary parameters to be determined, ω is the eigenfrequency associated with (m, n) th eigenmode, and $\lambda=m\pi/a$ and $\mu=n\pi/b$.

Substituting Eqs. (19) into Eq. (18), the analytical solutions can be obtained from

$$([K]-\omega^2[M])\{\Delta\}=\{0\} \quad (23b)$$

where $\{\Delta\}=\{U, V, W_b, W_s\}^t$, [C] and [M] refers to the flexural stiffness and mass matrices and ω to the corresponding frequency

$$[K]=\begin{bmatrix} a_{11} & a_{12} & a_{13} & a_{14} \\ a_{12} & a_{22} & a_{23} & a_{24} \\ a_{13} & a_{23} & a_{33} & a_{34} \\ a_{14} & a_{24} & a_{34} & a_{44} \end{bmatrix}, \quad [M]=\begin{bmatrix} m_{11} & 0 & 0 & 0 \\ 0 & m_{22} & 0 & 0 \\ 0 & 0 & m_{33} & m_{34} \\ 0 & 0 & m_{34} & m_{44} \end{bmatrix} \quad (24)$$

in which

$$a_{11}=A_{11}\lambda^2+A_{66}\mu^2, \quad a_{12}=\lambda\mu(A_{12}+A_{66}) \quad (25)$$

$$a_{13}=-\lambda[B_{11}\lambda^2+(B_{12}+2B_{66})\mu^2]$$
$$a_{14}=-\lambda[B_{11}^s\lambda^2+(B_{12}^s+2B_{66}^s)\mu^2]$$
$$a_{22}=A_{66}\lambda^2+A_{22}\mu^2$$
$$a_{23}=-\mu[(B_{12}+2B_{66})\lambda^2+B_{22}\mu^2]$$
$$a_{24}=-\mu[(B_{12}^s+2B_{66}^s)\lambda^2+B_{22}^s\mu^2]$$
$$a_{33}=D_{11}\lambda^4+2(D_{12}+2D_{66})\lambda^2\mu^2+D_{22}\mu^4$$
$$a_{34}=D_{11}^s\lambda^4+2(D_{12}^s+2D_{66}^s)\lambda^2\mu^2+D_{22}^s\mu^4$$
$$a_{44}=H_{11}^s\lambda^4+2(H_{12}^s+2H_{66}^s)\lambda^2\mu^2+H_{22}^s\mu^4+A_{55}^s\lambda^2+A_{44}^s\mu^2$$
$$m_{11}=m_{22}=I_1$$
$$m_{33}=I_1+I_3(\lambda^2+\mu^2)$$
$$m_{34}=I_1+I_5(\lambda^2+\mu^2)$$
$$m_{44}=I_1+I_6(\lambda^2+\mu^2)$$

3. Results and discussion

In numerical analysis, static and free vibration analysis of simply supported FG Plates is evaluated. The FG plate is taken to be made of aluminum and alumina with the following material properties:

Ceramic (P_C: Alumina, Al_2O_3): E_c=380 GPa; ν=0.3; ρ_c=5700 kg/m^3

Metal (P_M: Aluminium, Al): E_m=70 GPa; ν=0.3; ρ_m=2702 kg/m^3

And their properties change through the thickness of the plate according to power-law. The bottom surfaces of the FG plate are aluminum rich, whereas the top surfaces of the FG plate are alumina rich.

3.1 Free vibration analysis

The accuracy of the present theory is also evaluated through free vibration analysis of the FGM plates. Table 1 present Comparison of the first eight nondimensional frequency $\bar{\omega}=\omega a^2\sqrt{\rho_0 h/G}$ of simply supported homogeneous isotropic square plate versus thickness-to-lengh ratio h/a. As it can be seen, with increases of thickness-to-lengh ratio the nondimensional frequency decreases. Again the present results show good agreement with those reported by Hosseini *et al.* (2011), Thai *et al.* (2012) and 3-D Ritz.

As another verification attempt, Comparison study of frequency parameters $\bar{\omega}=\omega h\sqrt{\rho/G}$ rectangular plates when thickness-to-lengh ratio h/a=0.1 are presented in Table 2. It can be seen that the obtained results are in very good agreement with those predicted by Exact HSDT

Table 1 Comparison of the first eight nondimensional frequency $\bar{\omega} = \omega a^2 \sqrt{\rho_0 h / G}$ of simply supported homogeneous isotropic square plate $a=b$, $k=0$

h/a	Method	Modes							
		1	2	3	4	5	6	7	8
0.01	3-D Ritz	19.7392	49.3480	49.3480	78.9568	98.6951	98.6951	128.3030	128.3030
	Hosseini (2011)	19.7320	49.3032	49.3032	78.8421	98.5169	98.5169	128.0024	128.0024
	Thai (2012)	19.7320	49.3032	49.3032	78.8421	98.5169	98.5169	128.0024	128.0024
	Present	19.7320	49.3031	49.3031	78.8421	98.5170	98.5170	128.0025	128.0025
0.1	3-D Ritz	19.0898	45.6193	45.6193	70.1038	85.4876	85.4876	107.3710	107.3710
	Hosseini (2011)	19.0653	45.4869	45.4869	69.8093	85.0646	85.0646	106.7350	106.7350
	Thai (2012)	19.0653	45.4869	45.4869	69.8093	85.0646	85.0646	106.7350	106.7350
	Present	19.0656	45.4895	45.4895	69.8159	85.0749	85.0749	106.7523	106.7523
0.2	3-D Ritz	17.5264	38.4826	38.4826	55.7870	65.9961	65.9961	-	-
	Hosseini (2011)	17.4523	38.1883	38.1883	55.2543	65.3135	65.3135	78.9865	78.9865
	Thai (2012)	17.4523	38.1883	38.1883	55.2543	65.3135	65.3135	78.9865	78.9865
	Present	17.4539	38.1983	38.1983	55.2788	65.3506	65.3506	79.0464	79.0464
0.3	3-D Ritz	15.6877	31.9834	31.9834	44.5346	50.4850	50.4850	-	-
	Hosseini (2011)	15.5745	31.6413	31.6413	44.0236	51.1314	51.1314	60.6549	60.6549
	Thai (2012)	15.5744	31.6413	31.6413	44.0236	51.1314	51.1314	60.6551	60.6551
	Present	15.5780	31.6618	31.6618	44.0711	51.2016	51.2016	60.7649	60.7649

Table 2 Comparison study of frequency parameters $\bar{\omega} = \omega h \sqrt{\rho / G}$ rectangular plates when, $h/a=0.1$

(m, n)	Exact HSDT	Exact 3-D	FEM (HSDT)	Hosseini (2011)	Present
(1, 1)	0.0931	0.0932	0.0930	0.0930	0.0978
(2, 1)	0.2222	0.226	0.2222	0.2222	0.2333
(2, 2)	0.3411	0.3421	0.3406	0.3406	0.3581
(1, 3)	0.4158	0.4171	0.4149	0.4151	0.4364
(2, 3)	0.5221	0.5239	0.5206	0.5210	0.5476
(1, 4)	0.6545	-	0.6520	0.6525	0.6862
(3, 3)	0.6862	0.6889	0.6834	0.6840	0.7193
(2, 4)	0.7481	0.7511	0.7447	0.7454	0.7839
(3, 4)	0.8949	-	0.8896	0.8908	0.9370
(1, 5)	0.9230	0.9268	0.9174	0.9187	0.9663
(2, 5)	1.0053	-	0.9984	1.0001	1.0520
(4, 1)	1.0847	1.0889	1.0760	1.0001	0.6862
(3, 5)	1.1361	-	1.1266	1.1292	1.1880

(1985), Exact 3-D (1970), FEM (HSDT) and Hosseini *et al.* (2011).

The effect of side-to-thickness ratio on the fundamental frequencies of the FGM plate for different values of gradient index and aspect ratio are presented in Figs. 2 and 3, respectively. It's clear that the fundamental frequency is maximum when the gradient index $k=0$ and aspect ratio $a/b=2$, and minimum when the gradient index $k=10$ and aspect ratio $a/b=0.5$.

Figs. 4 and 5, plot the variation of the fundamental

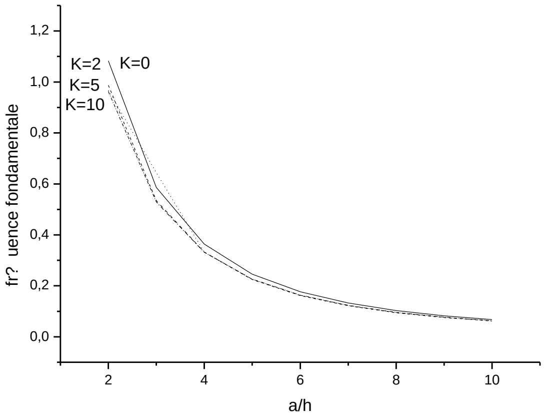

Fig. 2 Variation of fundamental frequencies versus side to thickness ratio of the FGM plate

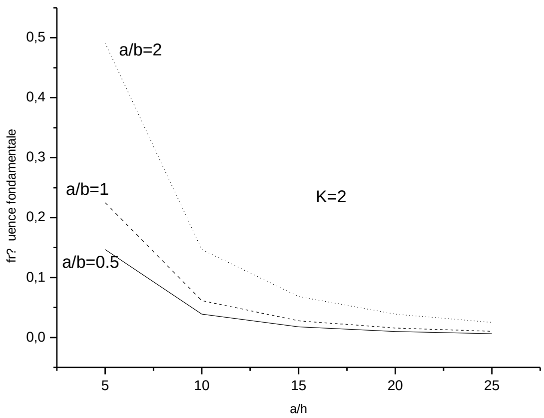

Fig. 3 Variation of fundamental frequencies versus side to thickness ratio of the FGM plate

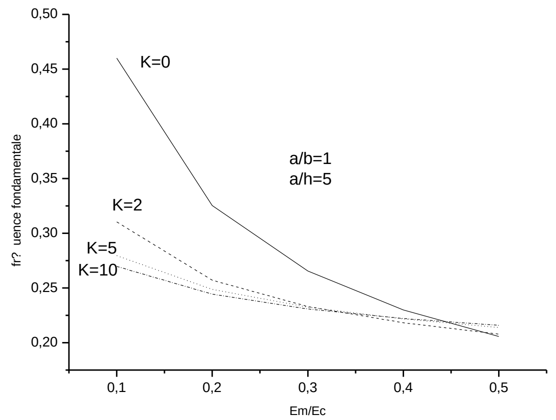

Fig. 4 Variation of fundamental frequencies versus E_m/E_c ratio of the FGM plate

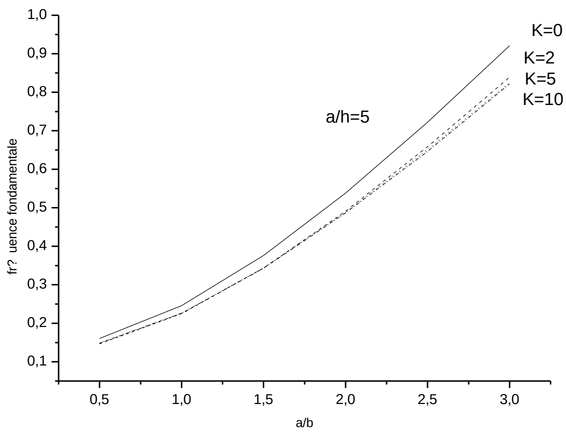

Fig. 5 Variation of fundamental frequencies versus aspect ratio of the FGM plate

frequencies of the FGM plate versus E_m/E_c and aspect ratio, respectively. As it can be seen, the difference of the fundamental frequencies increases as the aspect ratio increases.

4. Conclusions

In this work, a refined plate theory based on the refined shear deformation plate theory is successfully developed for free vibration simply supported FG plates. The theory accounts for a quadratic variation of the transverse shear strains across the thickness, and satisfies the zero traction boundary conditions on the top and bottom surfaces of the plate without using shear correction factors. Accuracy and convergence of the present refined plate theories was verified by comparing the results obtained with those reported in the literature for the FG plate. Parametric studies for varying of the power low index, the aspect and side-to-thickness ratio are discussed and demonstrated through illustrative numerical examples.

References

Ahouel, M., Houari, M.S.A., Adda Bedia, E.A. and Tounsi, A. (2016), “Size-dependent mechanical behavior of functionally graded trigonometric shear deformable nanobeams including neutral surface position concept”, *Steel Compos. Struct.*, **20**(5), 963-981.

Ait Amar Meziane, M., Abdelaziz, H.H. and Tounsi, A. (2014), “An efficient and simple refined theory for buckling and free vibration of exponentially graded sandwich plates under various boundary conditions”, *J. Sandw. Struct. Mater.*, **16**(3), 293-318.

Ait Yahia, S., Ait Atmane, H., Houari, M.S.A. and Tounsi, A. (2015), “Wave propagation in functionally graded plates with porosities using various higher-order shear deformation plate theories”, *Struct. Eng. Mech.*, **53**(6), 1143-1165.

Al-Basyouni, K.S., Tounsi, A. and Mahmoud, S.R. (2015), “Size dependent bending and vibration analysis of functionally graded micro beams based on modified couple stress theory and neutral surface position”, *Compos. Struct.*, **125**, 621-630.

Attia, A., Tounsi, A., Adda Bedia, E.A. and Mahmoud, S.R. (2015), “Free vibration analysis of functionally graded plates with temperature-dependent properties using various four variable refined plate theories”, *Steel Compos. Struct.*, **18**(1), 187-212.

Bakora, A. and Tounsi, A. (2015),” Thermo-mechanical post-buckling behavior of thick functionally graded plates resting on elastic foundations”, *Struct. Eng. Mech.*, **56**(1), 85-106.

Belabed, Z., Houari, M.S.A., Tounsi, A., Mahmoud, S.R. and Anwar Bég, O. (2014), “An efficient and simple higher order shear and normal deformation theory for functionally graded material (FGM) plates”, *Composites: Part B*, **60**, 274-283.

Beldjelili, Y., Tounsi, A. and Mahmoud, S.R. (2016), “Hygro-thermo-mechanical bending of S-FGM plates resting on variable elastic foundations using a four-variable trigonometric plate theory”, *Smart Struct. Syst.*, **18**(4), 755-786.

Belkorissat, I., Houari, M.S.A., Tounsi, A., Adda Bedia, E.A. and Mahmoud, S.R. (2015), “On vibration properties of functionally graded nano-plate using a new nonlocal refined four variable model”, *Steel Compos. Struct.*, **18**(4), 1063-1081.

Bellifa, H., Benrahou, K.H., Hadji, L., Houari, M.S.A. and Tounsi, A. (2016), “Bending and free vibration analysis of functionally graded plates using a simple shear deformation theory and the concept the neutral surface position”, *J Braz. Soc. Mech. Sci. Eng.*, **38**(1), 265-275.

Bennoun, M., Houari, M.S.A. and Tounsi, A. (2016), “A novel five variable refined plate theory for vibration analysis of functionally graded sandwich plates”, *Mech. Adv. Mater. Struct.*, **23**(4), 423-431.

Bouderba, B., Houari, M.S.A. and Tounsi, A., (2013) “Thermomechanical bending response of FGM thick plates resting on Winkler–Pasternak elastic foundations”, *Steel Compos. Struct.*, **14**(1), 85-104.

Bouderba, B., Houari, M.S.A. and Tounsi, A., Mahmoud, S.R. (2016), “Thermal stability of functionally graded sandwich plates using a simple shear deformation theory”, *Struct. Eng. Mech.*, **58**(3), 397-422.

Boukhari, A., Ait Atmane, H., Tounsi, A., Adda Bedia, E.A. and Mahmoud, S.R. (2016), “An efficient shear deformation theory for wave propagation of functionally graded material plates”, *Struct. Eng. Mech.*, **57**(5), 837-859.

Bounouara, F., Benrahou, K.H., Belkorissat, I. and Tounsi, A. (2016), “A nonlocal zeroth-order shear deformation theory for free vibration of functionally graded nanoscale plates resting on elastic foundation”, *Steel Compos. Struct.*, **20**(2), 227-249.

Bourada, M., Kaci, A., Houari, M.S.A. and Tounsi, A. (2015), “A new simple shear and normal deformations theory for functionally graded beams”, *Steel Compos. Struct.*, **18**(2), 409-423.

Bousahla, A.A., Houari, M.S.A., Tounsi, A. and Adda Bedia, E.A. (2014), “A novel higher order shear and normal deformation theory based on neutral surface position for bending analysis of advanced composite plates", *Int. J. Comput. Method*, **11**(6), 1350082.

Fekrar, A., El Meiche, N., Bessaim, A., Tounsi, A. and Adda Bedia, E.A. (2012), "Buckling analysis of functionally graded hybrid composite plates using a new four variable refined plate theory", *Steel Compos. Struct.*, **13**(1),91-107.

Hadji, L., Hassaine Daouadji, T., Ait Amar Meziane, M. and Tlidji, Y. (2016a), "Analysis of functionally graded beam using a new first-order shear deformation theory", *Struct. Eng. Mech.*, **57**(2), 315-325.

Hadji, L., Hassaine Daouadji, T. and Adda Bedia, E.A. (2016b), "Dynamic behavior of FGM beam using a new first shear deformation theory", *Earthq. Struct.*, **10**(2), 451-461.

Hadji, L., Zouatnia, N. and Kassoul, A. (2016c), "Bending analysis of FGM plates using a sinusoidal shear deformation theory", *Wind Struct.*, **23**(6), 543-558.

Hamidi, A., Houari, M.S.A., Mahmoud, S.R. and Tounsi, A. (2015), "A sinusoidal plate theory with 5-unknowns and stretching effect for thermomechanical bending of functionally graded sandwich plates", *Steel Compos. Struct.*, **18**(1), 235-253.

Hebali, H., Tounsi, A., Houari, M.S.A., Bessaim, A. and Adda Bedia, E.A. (2014), "A new quasi-3D hyperbolic shear deformation theory for the static and free vibration analysis of functionally graded plates", *J. Eng. Mech.*, ASCE, **140**(2), 374-383.

Hosseini-Hashemi, S., Fadaee, M. and Rokni Damavandi Taher, H. (2011), "Exact solutions for free flexural vibration of Levy-type rectangular thick plates via third-order shear deformation plate theory", *Appl. Math. Model.*, **35**(2), 708-727.

Larbi Chaht, F., Kaci, A., Houari, M.S.A., Tounsi, A., Anwar Bég, O. and Mahmoud, S.R. (2015), "Bending and buckling analyses of functionally graded material (FGM) size-dependent nanoscale beams including the thickness stretching effect", *Steel Compos. Struct.*, **18**(2), 425-442.

Mahi, A., Adda Bedia, E.A. and Tounsi, A. (2015), "A new hyperbolic shear deformation theory for bending and free vibration analysis of isotropic, functionally graded, sandwich and laminated composite plates", *Appl. Math. Model.*, **39**(9), 2489-2508.

Nedri, K., El Meiche, N. and Tounsi, A. (2014), "Free vibration analysis of laminated composite plates resting on elastic foundations by using a refined hyperbolic shear deformation theory", *Mech. Compos. Mater.*, **49**(6), 641-650.

Thai, H.T. and Choi, D.H. (2012), "A refined shear deformation theory for free vibration of functionally graded plates on elastic foundation", *Compos.: Part B*, **43**(5), 2335-2347.

Thai, H.T. and Kim, S.E. (2013a), "A simple quasi-3D sinusoidal shear deformation theory for functionally graded plates", *Compos. Struct.*, **99**, 172-180.

Thai, H.T. and Kim, S.E. (2013b), "A simple higher-order shear deformation theory for bending and free vibration analysis of functionally graded plates", *Compos. Struct.*, **96**, 165-173.

Tai, H.T., Nguyen, T.K. and Vo, T.P. (2014), "Analysis of functionally graded sandwich plates using a new first-order shear deformation theory", *Eur. J. Mech. A/Solids*, **45**, 211-225.

Tounsi, A., Houari, M.S.A., Benyoucef, S. and Adda Bedia, E.A. (2013), "A refined trigonometric shear deformation theory for thermoelastic bending of functionally graded sandwich plates", *Aerospace Sci. Tech.*, **24**(1), 209-220.

Zemri, A., Houari, M.S.A., Bousahla, A.A. and Tounsi, A. (2015), "A mechanical response of functionally graded nanoscale beam: an assessment of a refined nonlocal shear deformation theory beam theory", *Struct. Eng. Mech.*, **54**(4), 693-710.

Zhang, D.G. (2013), "Modeling and analysis of FGM rectangular plates based on physical neutral surface and high order shear deformation theory", *Int. J. Mech. Sci.*, **68**, 92-104.

Zidi, M., Tounsi, A., Houari, M.S.A., Adda Bedia, E.A. and Anwar Bég, O. (2014), "Bending analysis of FGM plates under hygro-thermo-mechanical loading using a four variable refined plate theory", *Aero. Sci. Technol.*, **34**, 24-34.

CC